Photo-thermal response in dual-gated bilayer graphene

M.-H. Kim,[1] J. Yan,[1,2] R. J. Suess,[3] T. E. Murphy,[3] M. S. Fuhrer,[1] and H. D. Drew[1]

[1] *Center for Nanophysics and Advanced Materials, Department of Physics, University of Maryland, College Park, Maryland 20742, USA*
[2] *Physics Department, University of Massachusetts, Amherst, MA 01002, USA*
[3] *Institute for Research in Electronics and Applied Physics, University of Maryland, College Park, Maryland 20742, USA*

The photovoltaic and bolometric photoresponse in gapped bilayer graphene was investigated by optical and transport measurements. A pulse coincidence technique at 1.5 μm was used to measure the response times as a function of temperature. The bolometric and photovoltaic response times were found to be identical implying that the photovoltaic response is also governed by hot electron thermal relaxation. Response times of $\tau \sim 100$ - 20 ps were found for temperatures from 3 - 100 K. Above 10 K, the relaxation time was observed to be $\tau = 25 \pm 5$ ps, independent of temperature within noise.

There is growing recognition that graphene has exceptional potential as a new optoelectronic material, which has led to a flurry of recent research activity and rapid advances. [1–3] Graphene's unique massless band structure gives rise to direct transitions and strong (specific) coupling to light at all wavelengths, [4] and ultra-fast response (from nanosecond to femtosecond) [4] room temperature operation for many applications. A photovoltaic response has been observed for visible light and we have recently observed both photovoltaic and bolometric response in bilayer graphene at THz frequencies. [5] Diode-like rectification behavior is observed with contacts to dissimilar metals. [1, 2, 5, 6] However, the mechanism of the photovoltaic response has not been definitively identified. Both p-n junction physics similar to conventional semiconductor photovoltaic sensors and a thermoelectric mechanism remain viable possibilities. In a recent study we observed a hot electron bolometric response in bilayer graphene, which highlighted the outstanding thermal properties of graphene. [5] Therefore, understanding the role of hot electron effects in the photoresponse of graphene is critical to the development of graphene-based optoelectronic devices such as bolometers and photovoltaic sensors. [7]

Excited electrons in graphene thermalize quickly on the femtosecond time scales [8, 9] by electron-electron scattering. [10] These hot electrons transfer their thermal energy to the graphene lattice by the emission of phonons on a much longer time scale because of the weak electron-phonon interaction. [10–13] The thermal relaxation of hot electrons by optical phonons [9, 14, 15] and by acoustic phonons [5, 16] has received much recent attention. The processes of cooling by optical and acoustic phonons are clearly distinguishable because their thermal timescales differ by a few orders of magnitude. High pulse energy radiation produces hot electrons with energies above the optical phonon energy (~ 200 meV) that cool by optical phonon emission in a timescale of a few picoseconds. [9, 14, 15] For longer times and/or lower pulse energy radiation, acoustic phonon assisted cooling is dominant with sub-nanosecond timescales. [5, 16]

Hot electrons can be utilized for bolometric and photovoltaic photoresponse detection. [5, 7, 17] The bolometric response makes use of the temperature dependence of the resistivity, which is significant in gapped bilayer graphene. On the other hand, the hot electrons can also give rise to a photo-thermoelectric response. Diffusion of heat and carriers to the contacts produce a thermoelectric response. A competing mechanism for photovoltaic response is charge separation by the built-in electric fields at metal-graphene junctions due to proximity doping. It remains unclear which of these two mechanisms dominates in graphene photovoltaic devices.

In this paper, we use electrical transport and optical photoresponse measurements to characterize the bolometric and photovoltaic response of a dual-gated bilayer graphene device. The temperature-dependent resistance of the device which allows a bolometric response is characterized both optically and with AC transport measurements, which together establish that the response is thermal. We found that light also generates a voltage across the sample with zero bias current. We compare this photovoltaic response with the well-understood bolometric signal in the same device as functions of dual-gate voltages and temperature. In particular pulse coincidence measurement reveals that the photo voltage displays the same temperature-dependent relaxation time as the bolometric response, demonstrating that diffusive hot carrier relaxation in graphene dominates the observed photo voltage of the device.

The bilayer graphene device we studied was fabricated by mechanical exfoliation of natural graphite on a resistive silicon wafer (200 Ωcm) which was ion implanted with boron and annealed to provide a highly conducting but transparent back-gate at cryogenic temperatures. A 300 nm thick SiO_2 layer was grown by a dry oxidation process from the silicon wafer. A micrograph of the device is shown in Fig. 1(a) inset and schematic of device geometry is shown in Fig. 1(b) inset. A thin Nichrome film was used as a semitransparent top-gate. Details of

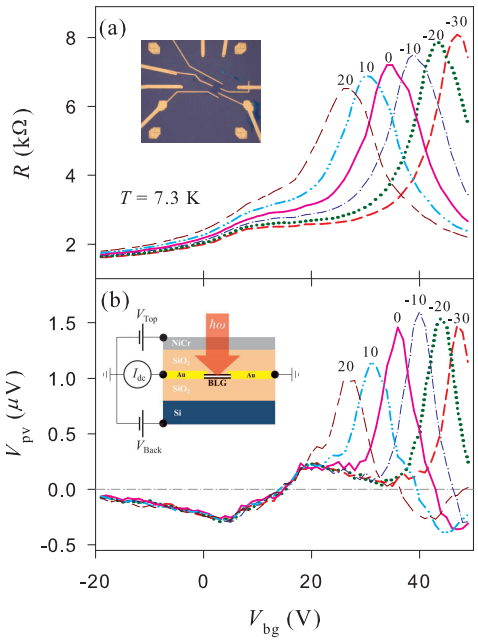

FIG. 1. **Photovoltaic response and resistance of a dual-gated bilayer graphene.** (a) Resistance and (b) photovoltaic response as a function of back gate voltage for different top gate voltage at T = 7.3 K and zero bias current. Inset in (a) shows an optical micrograph of the bilayer graphene device. Inset in (b) shows schematic of device geometry and electric-field-effect gating.

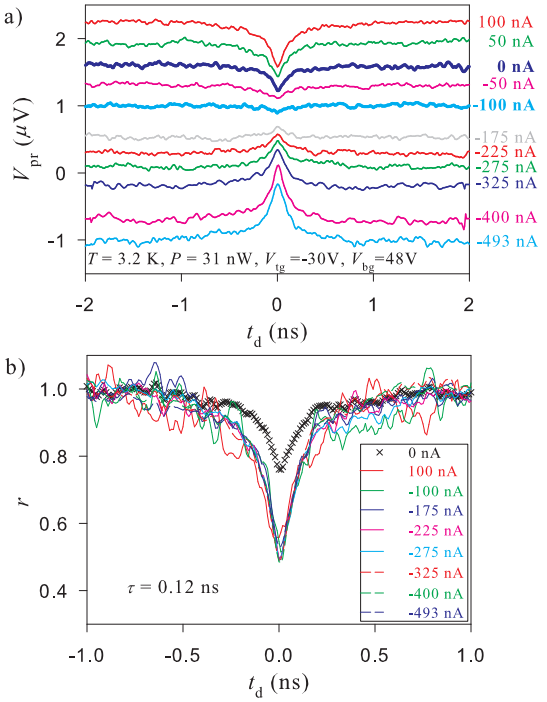

FIG. 2. **Bias current dependence of the pump-probe measurements.** Photoresponse from pump-probe laser pulses as a function of time delay t_d at 3.2 K and laser absorbed power of 31 nW. The sample is gated to charge neutrality with V_{tg} = -30 V, V_{bg} = 48 V. (a) Bias current I_{dc} dependence of probe-induced photoresponse voltage $V_{pr}(t_d)$. The I_{dc} = 0 curve is the photovoltaic response. (b) r is normalized bolometric response $\Delta V(I_{dc}) = V(I_{dc}) - V(0)$ and photovoltaic response $V(0)$. $r = V_{pr}(t_d)/V^0_{pv}$, where $V^0_{pv} = V_{pv}(t_d \gg \tau)$. The thermal response time τ is defined as the half-width at half-maximum of the dip. All dips have a similar time constant $\tau = 0.12 \pm 0.01$ ns.

the device structure and the gating scheme can be found in Ref. 5. The dual-gated structure allows for independent tuning of carrier density and bandgap of the bilayer graphene device. Figure 1(a) shows the device resistance R at 7.3 K as a function of back gate voltage V_{bg} at various top gate voltages V_{tg}. A broad resistance peak appears near V_{bg} = 10 V independent of V_{tg} and is attributed to the part of the bilayer device that is not gated by the top gate. [18] The other sharper peak shifts with V_{tg} and is attributed to dual-gated device region.

The photoresponse and sample resistance were measured simultaneously. The photoresponse shown in Fig. 1(b) was measured with bias current I_{dc} = 0 which gives the photovoltaic response V_{pv}. At V_{bg} = 10 V where the broad peak of R occurs, V_{pv} also doesn't depend on V_{tg}, and V_{pv} crosses zero at $V_{bg} \approx$ 15 V. This behavior is similar to that observed in photo-thermoelectric results reported in graphene. [7, 15, 19] For $V_{bg} >$ 20V, V_{pv} depends on both V_{tg} and V_{bg}, and reaches a maximum value at the maximum R.

To measure the response times of these signals we used a pulse coincidence technique. The photoresponse was studied at 1.56 μm with a pulsed laser with a 65-fs pulse width and 100 MHz repetition rate. Pulses from two fiber lasers are locked together with a tunable time separation at repetition rate near 100 MHz (Menlo Systems), which allows pulse coincidence measurements with precise time delays from a few ps to 10 ns without a mechanical delay line. The absorption of 1.56 μm radiation in the graphene was estimated to be 1.2% by considering effects due to the silicon substrate and the Nichrome top gate. [5] The graphene absorbs an average power of 0.37 nW from the pump and probe pulses and generates a temperature rise ΔT, which can be measured using the temperature dependence of R.

The dependence of the photoresponse with pulse time delay for different bias currents is shown in Fig. 2(a) under conditions that the device is gated to its charge neutral point. At zero bias current the signal is purely photovoltaic. For non-zero bias there is also a bolometric signal given by $V_b = I_{dc}\Delta R$ which was reported earlier. [5] We find that the total photoresponse can be described as $V_{pr}(I_{dc}) = V_b(I_{dc}) + V_{pv}$ allowing a separation of the photovoltaic and bolometric contributions. Therefore the bolometric response can be obtained from $V_b(I_{dc}) = V_{pr}(I_{dc}) - V_{pr}(0)$. It is seen in the figure that this bolometric response is dominant except near I_{dc} = 0

where the response is purely photovoltaic.

These pulse time delay data allow a measurement of the response time τ of the two components of the photoresponse. For long pulse delay times, t_d, average probe-pulse induced photo voltage, V_{pr} does not change with respect to the time delay t_d. When the delay is short ($t_d < \tau$), however, the magnitude of V_{pr} is reduced due to the nonlinear radiation power dependence of the response so that the photo voltage $V_{pr}(t_d)$ displays a peak or dip at $t_d = 0$. The magnitude of this peak or dip increases with the non-linear power dependence of V_{pr}.

Figure 2(b) shows V_{pv} and $V_b(I_{dc})$ normalized to the response in the absence of the pump pulse for several different I_{dc}. All of the normalized V_b for different I_{dc} collapse to one curve because the small Joule heating $I_{dc}^2 R$ does not significantly raise the electron temperature above the lattice temperature. Both bolometric and photovoltaic responses produce a narrow dip with a sub-nanosecond width at zero time delay when the pump and probe pulses are coincident. Surprisingly, the widths of both bolometric and photovoltaic dips are seen to be the same to within the experimental error. The time constants determined by the half widths at half maximum of the dips are 0.12 ± 0.01 ns. This demonstrates that both V_{pv} and $V_b(I_{dc})$ have the same response time and since the bolometric response is clearly thermal [5] this implies that the photovoltaic response is also thermal. Similar results are observed at $V_{tg} = 0$ V and $V_{bg} = 30$ V for temperatures below 10 K.

To gain further insight into the nature of the photo voltage, we measured its gate voltage dependence. Figure 3 shows back gate voltage dependence of photo voltage at $T = 15$ K with $V_{tg} = 0$ and $I_{dc} = 0$. As can be seen from the data in Fig. 1(a), the top gate does not gate the entire device. To obtain uniform gating we control only the back gate voltage with zero top gate voltage. Figures 3(a) and (b) display the photovoltaic response below and above the maximum V_{pv} observed at around $V_{bg} = 25$ V. The peak or dip structure is associated with the sign of V_{pv}, and its depth or height depends on the nonlinear power dependence of V_{pv}. Both sign and power nonlinearity depend on back gate voltage. For example, at $V_{bg} = 15.5$ V the response $V_{pv}(t_d)$ is independent of t_d indicating that V_{pv} is linear with radiation power. As the power nonlinearity of V_{pv} grows above or below $V_{bg} = 15.5$ V, the dip or peak of V_{pv} appears and grows. Remarkably, however, all of the pump-probe data have the same $\tau = 25$ ps ± 5 ps. The gate-independent time constant shows that the photovoltaic response is thermal at all gate voltages not only at maximum R with respect to V_{bg} as shown in Fig. 2(b) where it could be directly compared with the bolometric response. This observation demonstrates that the photovoltaic response time in bilayer graphene is the intrinsic thermal time constant of hot electron energy relaxation.

We also measured the temperature dependence of the

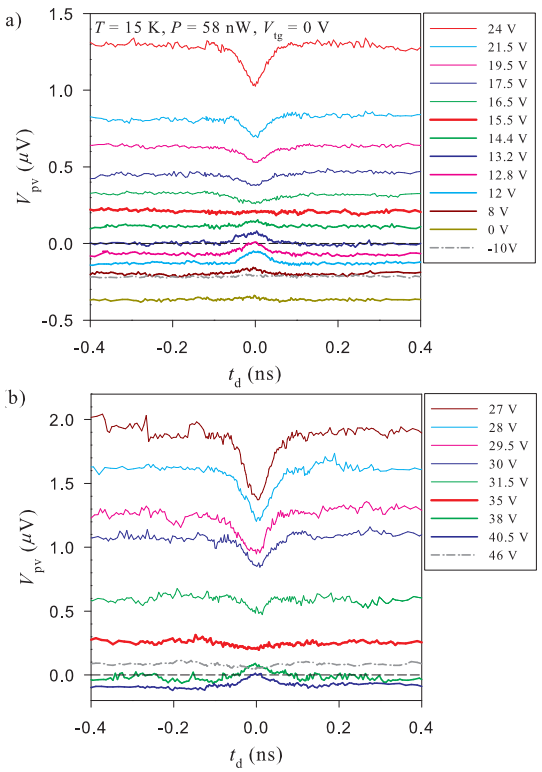

FIG. 3. **Gate voltage dependence of the pump-probe measurements.** Pump-probe pulse induced photovoltaic response as a function of time delay at 15 K and laser power of 58 nW. $I_{dc} = 0$. The data was taken at several back gate voltages V_{bg} with zero top gate voltage (a) below and (b) above $V_{bg} = 25$ V where the maximum photovoltaic response is found. The thin dashed line at $V_{bg} = 0$ is a guide line. All cusps have the same thermal time constant $\tau = 25 \pm 5$ ps within error.

response time in our graphene device. Figure 4 exhibits τ obtained from the photovoltaic response in the temperature range 3 K - 87 K at several different dual-gate voltages. The response time for different gate voltages coincides within error as shown in Fig. 4. The time constant decreases from ~ 80 ps at 3 K to ~ 20 ps at 80 K. Above $T \sim 10$ K, τ is seen to be temperature independent to within experimental error.

The thermal relaxation rate is given by the ratio of the electronic heat capacity C to thermal conductance G. The thermal conductance was obtained using transport measurements as described in Ref. 5. For $T < 8$ K, the transport measurements gives $G = 0.5 \times (T/5)^{3.45}$ nW/K which is in reasonable agreement with the value estimated for cooling by acoustic phonons. [13] A crossover of the thermal conductance from T^3 to linear T is predicted for $T > T_{BG}$, where T_{BG} is the Bloch-Grünheisen temperature given by $k_B T_{BG} \approx 2\hbar v_s k_F$. [13] Assuming a sound velocity $v_s = 2.6 \times 10^4$ m/s [20] and a disorder-induced charge density of $n_{\rm rms} \sim 10^{12}$ cm^{-2} [21], we find $T_{BG} \sim 70$ K. Although our sample is nominally charge

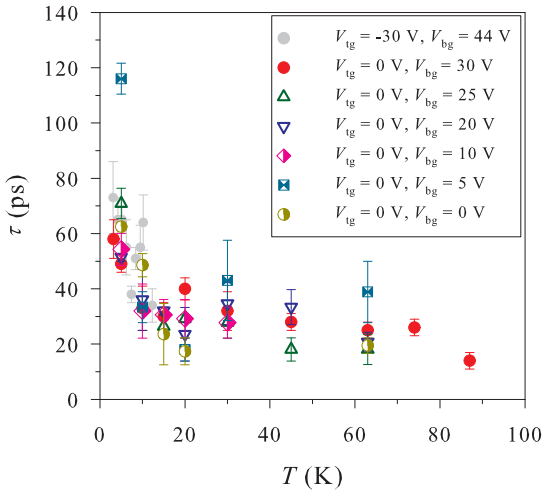

FIG. 4. **Temperature dependence of thermal response time.** Thermal time constant τ of the photovoltaic response vs. temperature measured by the pulse coincidence technique for several different dual-gate voltage settings.

neutral at $R_{\max}$, it is widely accepted that disorder creates electron-hole puddles [22] and thus T_{BG} is nonzero at all gate voltages. Transport measurements show that the Bloch-Grünheisen regime behavior occurs for $T < 0.2T_{BG} \sim 14$ K. [20] The behavior of G and C above $T \sim 0.2T_{BG}$ may be complicated by disorder induced supercollision cooling [16, 23] and/or the non-parabolic band structure of gapped bilayer graphene [4] which leads to small Fermi energies. We measured $G = 0.91 \times T^{1.04}$ nW/K for $T > 8$ K, which is reasonable in view of these considerations.

On the other hand, diffusion cooling of hot electrons also gives a linear T dependent thermal conductance. Diffusion cooling provides a thermal conductance $k = \Lambda T/R_g$, by the Wiedermann-Franz law, where $\Lambda = 24.4$ nWΩ/K^2 is the Lorentz number, and R_g is bilayer graphene resistance. At the peak resistance for our sample, $k = 3.4 \times 10^{-12} \times T^{1.0}$ W/K, which is two orders of magnitude smaller than the electron-phonon conductance. We conclude that acoustic phonon mediated cooling of hot electrons is dominant in our samples.

We note, however, that the thermoelectric and photovoltaic signals are a consequence of diffusion. For asymmetric contacts the thermal diffusion and charge flow at the two contacts differs leading to a net potential difference. The diffusion length $\xi = (k/G)^{1/2}$ is estimated to be 0.5 μm at 10 K which is much smaller than the sample size of 5 μm so that the sample temperature rise and response time is dominated by the thermal conductance to the lattice which greatly reduces the thermoelectric signals in these large area, low conductance samples. The thermoelectric effect produces an electric field $e = S\nabla T$, where S is the Seebeck coefficient and ∇T is the gradient of the temperature. The heat conductance to the lattice diminishes ∇T at the contact and therefore the thermoelectric field by a factor of $2\xi/L$ compared with pure diffusion.

At low temperatures ($k_BT < \mu$, where μ is the local Fermi energy in the graphene and k_B is the Boltzmann constant) the electronic specific heat is $C = \alpha T$, where $\alpha = (\pi^2/3)v(E_F)k_B^2$, where $v(E_F)$ is the density of states for bilayer graphene. In the parabolic band approximation of (ungapped) graphene $v(E_F) \approx \gamma_1/(\pi\hbar^2 v_F^2)$ where the interlayer coupling $\gamma_1 = 390$ meV [24], $v_F = 1 \times 10^6$ m/s is the monolayer graphene Fermi velocity. For our sample area of 25 μm^2, this gives $\alpha = 2.6 \times 10^{-20}$ J/K^2. Thus the thermal response time of our bilayer sample can be estimated $\tau = C/G \approx 29$ ps independent of temperature for $T > 8$ K which is in reasonable agreement with the measured τ shown in Fig. 4.

In summary, we have reported photovoltaic response time measurements on gapped bilayer graphene. The devices show both bolometric and photovoltaic responses, which were separated by their bias current dependence. The identical response time constants observed for the bolometric and photovoltaic responses as a function of gate voltages and temperature implies that both effects are governed by the same intrinsic hot electron-phonon thermal relaxation process. The observed response times of 10 - 100 ps indicates that hot electron relaxation occurs through acoustic phonon emission. These observations support the growing realization that graphene appears to have great promise for fast sensitive photo detectors over a wide spectral range.

The authors thank A. B. Sushkov, G. S. Jenkins, and D. C. Schmadel for helping with the optical cryostat setup and for valuable discussions. This work was supported by IARPA, the ONR MURI program and the NSF (grants DMR-0804976 and DMR-1105224) and in part by the NSF MRSEC (grant DMR-0520471).

[1] F. Xia, T. Mueller, Y.-M. Lin, A. Valdes-Garcia, and P. Avouris, Nature Nanotech. **4**, 839 (2009).
[2] T. Mueller, F. Xia, and P. Avouris, Nature Photonics **4**, 297 (2010).
[3] T. J. Echtermeyer, L. Britnell, P. K. Jasnos, A. Lombardo, R. V. Gorbachev, A. N. Grigorenko, A. K. Geim, A. C. Ferrari, and K. S. Novoselov, Nature Commun. **2**, 458 (2011).
[4] A. H. Castro Neto, F. Guinea, N. M. R. Peres, K. S. Novoselov, and A. K. Geim, Rev. Mod. Phys. **81**, 109 (2009).
[5] J. Yan, M.-H. Kim, J. A. Elle, A. B. Sushkov, G. S. Jenkins, H. M. Milchberg, M. S. Fuhrer, and H. D. Drew, Nature Nanotech. **7**, 472 (2012).
[6] B. Huard, N. Stander, J. A. Sulpizio, and D. Goldhaber-Gordon, Phys. Rev. B **78**, 121402 (2008).
[7] N. M. Gabor, J. C. W. Song, Q. Ma, N. L. Nair, T. Taychatanapat, K. Watanabe, T. Taniquchi, L. S. Levitov, 5

and P. Jarillo-Herrero, Science **334**, 648 (2011).
[8] P. A. George, J. Strait, J. Dawlaty, S. Shivaraman, M. Chandrashekhar, F. Rana, and M. G. Spencer, Nano Lett. **8**, 4248 (2008).
[9] C. H. Lui, K. F. Mak, J. Shan, and T. F. Heinz, Phys. Rev. Lett. **105**, 127404 (2010).
[10] W.-K. Tse, E. H. Hwang, and S. D. Sarma, Appl. Phys. Lett. **93**, 023128 (2008).
[11] J.-H. Chen, C. Jang, S. Xiao, M. Ishigami, and M. S. Fuhrer, Nature Nanotech. **3**, 206 (2008).
[12] R. Bistritzer and A. H.MacDonald, Phys. Rev. Lett. **102**, 206410 (2009).
[13] J. K. Viljas and T. T. Heikkilä, Phys. Rev. B **81**, 245404 (2010).
[14] J. H. Strait, H. Wang, S. Shivaraman, V. Shields, M. Spencer, and F. Rana, Nano Lett. **11**, 4902 (2011).
[15] D. Sun, G. Aivazian, A. M. Jones, J. S. Ross, W. Yao, D. Cobden, and X. Xu, Nature Nanotech. **7**, 114 (2012).
[16] M. W. Graham, S.-F. Shi, D. C. Ralph, J. Park, and P. L. McEuen, Nature Phys. AOP (2012), DOI:10.1038/nphys2493.
[17] J. C. W. Song, M. S. Rudner, C. M. Marcus, and L. S. Levitov, Nano Lett. **11**, 4688 (2011).
[18] J. Yan and M. S. Fuhrer, Nano Lett. **10**, 4521 (2010).
[19] X. Xu, N. M. Gabor, J. S. Alden, A. M. van der Zande, and P. L. McEuen, Nano Lett. **10**, 562 (2010).
[20] D. K. Efetov and P. Kim, Phys. Rev. Lett. **105**, 256805 (2010).
[21] J. Yan, E. A. Henriksen, P. Kim, and A. Pinczuk, Phys. Rev. Lett. **101**, 136804 (2008).
[22] J. Martin, N. Akerman, G. Ulbricht, T. Lohmann, J. H. Smet, K. von Klitzing, and A. Yacoby, Nature Phys. **4**, 144 (2008).
[23] J. C. W. Song, M. Y. Reizer, and L. S. Levitov, Phys. Rev. Lett. **109**, 106602 (2012).
[24] L. M. Zhang, Z. Q. Li, D. N. Basov, M. M. Fogler, Z. Hao, and M. C. Martin, Phys. Rev. B **78**, 235408 (2008).